NODAGATOC, a New Chelator-Coupled Somatostatin Analogue Labeled with [$^{67/68}$Ga] and [^{111}In] for SPECT, PET, and Targeted Therapeutic Applications of Somatostatin Receptor (hsst2) Expressing Tumors

Klaus-Peter Eisenwiener,[†,⊥] M. I. M. Prata,[‡,⊥] I. Buschmann,[†] Han-Wen Zhang,[†] A. C. Santos,[§] Sandra Wenger,[∥] Jean Claude Reubi,[∥] and Helmut R. Mäcke*[,†]

Division of Radiological Chemistry, Institute of Nuclear Medicine, Department of Radiology, University Hospital, Petersgraben 4, CH-4031 Basel, Switzerland, Departamento de Bioquímica e CNC, Universidade de Coimbra, Coimbra, Portugal, Faculdade de Medicina, Serviço de Biofísica, Universidade de Coimbra, Coimbra, Portugal, and Division of Cell Biology and Experimental Cancer Research, Institute of Pathology, University of Berne, PO Box 62, Murtenstrasse 31, CH-3010 Berne, Switzerland. Received August 10, 2001; Revised Manuscript Received December 27, 2001

A monoreactive NOTA (1,4,7-triazacyclononane-1,4,7-triacetic acid) derived prochelator (1-(1-carboxy-3-carbo-*tert*-butoxypropyl)-4,7-(carbo-*tert*-butoxymethyl)-1,4,7-triazacyclononane (NODAGA(tBu)$_3$)) was synthesized in five steps with an overall yield of 21%. It is useful for the coupling to the N-terminus of peptides on solid phase and in solution; it was coupled to [Tyr^3]-octreotide (TOC) on solid phase, and the resulting peptide, NODAGA-Tyr^3-octreotide (NODAGATOC), was labeled with the radiometals ^{111}In and ^{67}Ga in high yields and good specific activities. [^{67}Ga]− and [^{111}In]−NODAGA-Tyr^3-octreotide appear to be useful to visualize primary tumors and metastases which express somatostatin receptors subtype 2 (sstr2), such as neuroendocrine tumors, because of their high affinity to this receptor subtype with $IC_{50} = 3.5 \pm 1.6$ nM and 1.7 ± 0.2 nM, respectively. NODAGATOC could be used as a SPECT and PET tracer, when labeled with ^{111}In, ^{67}Ga, or ^{68}Ga, and even for therapeutic applications. Surprisingly, [^{111}In]−NODAGATOC shows 2 times higher binding affinity to sstr2, but also a factor of 4 higher affinity to sstr5 compared to [^{67}Ga]−NODAGATOC. [^{67}Ga]−NODAGATOC is very stable in serum and rat liver homogenate. There is no difference in the rate of internalization into AR4-2J rat pancreatic tumor cells; both radioligands are highly internalized, at 4 h a 3 times higher uptake compared to [^{111}In]−DOTA-Tyr^3-octreotide ([^{111}In]−DOTATOC) was found. The biodistribution of [^{67}Ga]−NODAGATOC in AR4-2J tumor bearing nude mice is very favorable at short times after injection; there is fast excretion from all nontarget organs except the kidneys and high uptake in sst receptor rich organs and in the AR4-2J tumor. Again it is superior to [^{111}In]−DOTATOC in this respect. The results indicate an improved biological behavior which is likely due to the fact that an additional spacer group separates the chelate from the pharmacophoric part of the somatostatin analogue.

INTRODUCTION

Peptides are important regulators of growth and cellular functions in normal tissue but also in tumors. Tumors often overexpress receptors for different regulatory peptides. Certain types of tumors also respond to the growth inhibiting or growth promoting signals of certain peptides. This effect has become important in the treatment of some tumors in man. An important example are analogues of SRIF[1] (somatostatin release inhibiting factor) which are being used in the treatment of symptomatic neuroendocrine tumors and in acromegaly (*1*). A development of the last 10 years or so has been the use of radiolabeled versions of regulatory peptide analogues in the in vivo localization of tumors (*2*−*8*). Of paramount importance is the DTPA-derivatized somatostatin analogue octreotide labeled with [^{111}In] which is commercially available under the trade name OctreoScan (*9*, *10*). As this type of peptide−chelate conjugates show very rapid blood clearance and diffusion into different tissues, the use of short-lived positron emitters becomes feasible. We have introduced a few strategies that use

* To whom correspondence should be addressed: Tel: ++41 61 265 46 99; Fax: ++41 61 265 55 59, E-mail: hmaecke@uhbs.ch.

† Institute of Nuclear Medicine.

‡ Departamento de Bioquímica e CNC, Universidade de Coimbra.

§ Faculdade de Medicina, Serviço de Biofísica, Universidade de Coimbra.

∥ University of Berne.

⊥ K.-P.E. and M.I.M.P contributed equally to these studies.

[1] Abbreviations: SRIF, somatotropin release inhibiting factor; sstr, somatostatin receptor; DIC, diisopropylcarbodiimide; DOTA, 1,4,7,10-tetraazadodecane-1,4,7,10 tetraacetic acid; DTPA, diethylenetriaminepentaacetic acid; octreotide, D-Phe-Cys-Phe-D-Trp-Lys-Thr-Cys-Thr(ol) (disulfide bond); NOTA, 1,4,7-triazacyclononane-1,4,7-triacetic acid; NMP, *N*-methylpyrrolidone; DFO, desferrioxamine; Fmoc, 9-fluorenylmethoxycarbonyl; TFA, trifluoroacetic acid; HATU, *O*-(7-azabenzotriazol-1-yl)-1,1,3,3-tetramethyluronium hexafluorophosphate; TMS, tetramethylsilane; FCS, foetal calf serum; DMEM, Dulbecco's minimal essential medium; MOPS, 3-morpholinopropanesulfonic acid; DIPEA, diisopropylethylamine; HEPES, *N*-(2-hydroxyethyl)-piperazine-*N*′-2-ethanesulfonic acid; Tris, tris(hydroxymethyl)-aminomethane; BSA, bovine serum albumine; TETA, 1,4,8,10-tetraazacyclotetradecane-1,4,8,10-tetraacetic acid.

10.1021/bc010074f CCC: $22.00
Published on Web 04/23/2002

[^{68}Ga], a 68 min half-life-generator-produced metallic positron emitter coupled to somatostatin analogues (*11*−*13*). Whereas the use of the bifunctional chelator desferrioxamine-B (DFO) led to a radiopeptide which showed very good tumor targeting and visualization in a tumor-bearing rat model, the same conjugate was not very successful in patients because of a slow blood clearance (*14*).

The DOTA monoamide conjugated peptide [Tyr^3]-octreotide (DOTA-Tyr^3-octreotide = DOTATOC) showed very promising in vitro and in vivo properties if labeled with ^{67}Ga, ^{111}In, and ^{90}Y (*11*, *15*). The IC_{50} value of Ga^{III}−DOTATOC, if measured in an assay using a sstr2 receptor expressing cell line, and [^{125}I]-[Leu^8, D-Trp^{22}, Trp^{25}]-somatostatin-28 was 2.5 ± 0.5 nM compared to 11.4 ± 1.7 nM of the corresponding Y^{III}−DOTATOC (*16*). In addition, a Scatchard analysis using rat brain cortex membranes gave a K_d value of 0.46 ± 0.1 nM for [^{67}Ga]−DOTATOC (*16*) and 2.57 ± 0.2 nM for [^{111}In]−DOTATOC, respectively (*15*). The uptake of the respective radioligands in a tumor-bearing mouse model (AR4-2J rat pancreatic tumor cell line) was 13% of the injected dose per g (%ID/g) tumor for [^{111}In]−DOTATOC and 30% ID/g tumor for [^{67}Ga]−DOTATOC at 4 h postinjection. Interestingly, the [^{67}Ga]−DOTATOC showed a lower uptake and shorter residence time in the kidney compared to [^{111}In]−DOTATOC. The respective radioactivities in the kidney at 1, 4, 24, and 48 h for [^{111}In]−DOTATOC were 15, 12.5, 8, and 4% ID/g, whereas for [^{67}Ga]−DOTATOC the radioactivities in the kidneys were 8.5, 7.5, 4, and 2.5% ID/g at the same time points (*11*).

The reason for these differences are not fully understood yet. The metal ion dependence may stem from structural differences within the coordination environment. The X-ray crystal structures of the model peptides Ga^{III}−DOTA-D-PheNH$_2$ and Y^{III}(In^{III}, manuscript in preparation)−DOTA-D-PheNH$_2$ showed remarkable differences. In the Ga^{III} complex, DOTA adopts a cis-pseudooctahedral geometry with a folded macrocyclic unit (2424 conformation) (Figure 1). The equatorial plane is formed by two transannular nitrogens of the macrocyclic ring and the oxygens of the corresponding carboxylate groups. The axial positions are occupied by the remaining two ring nitrogens. Two potential coordination sites of the chelator are free, namely one carboxylate group and the amide carboxy oxygen (*11*). This structural feature may contribute to the somewhat more efficient kidney clearance, and the latter leads to a spacer function between chelate and bioactive peptide (Figure 1). This may consequently introduce less steric strain and improve receptor binding affinity and concomitantly tumor uptake in vivo. Unlike the Ga^{III} structure in Y^{III}(In^{III})−DOTA-D-PheNH$_2$, the coordination number of Y^{III} (In^{III}) is eight and includes the amide carbonyl oxygen. This may lead to some steric scrambling and lower the receptor affinity compared to a chelate which is somewhat remote from the pharmacophoric part of the peptide as in the Ga^{III} complex.

The purpose of this study therefore is to synthesize a NOTA-based [Tyr^3]-octreotide derivative (NODAGA-Tyr^3-octreotide, NODAGATOC) which should allow to carry a spacer function between the ^{67}Ga (^{111}In) complexing chelator and the peptide. This should demonstrate the importance of the spacer for improved receptor binding affinity. The first step was the synthesis of a bifunctional NOTA-derived prochelator which can be conveniently coupled to peptides on solid support and in solution. In addition, we studied SRIF-receptor affinity, biodistribution as well as internalization and externalization of the ^{67}Ga (^{111}In) labeled peptide compared to our "gold standard" of somatostatin receptor scintigraphy [^{111}In]−DOTA-Tyr^3-octreotide in the rat pancreas tumor cell line AR4-2J and a corresponding nude mice tumor model. NOTA was used because of the known high stability of the Ga^{III}−NOTA and In^{III}−NOTA complexes which makes any interference and false interpretation of biological and pharmacological data due to a potential transchelation chemistry rather unlikely.

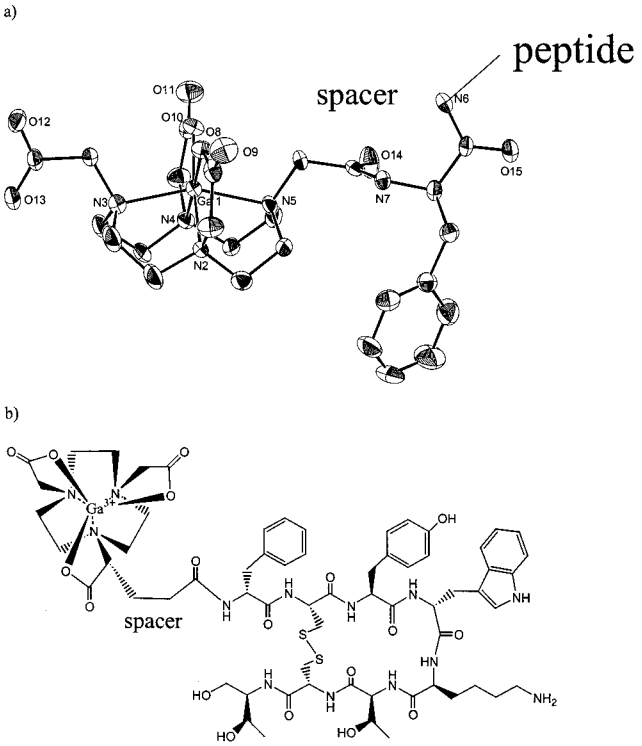

Figure 1. (a) ORTEP plot of the crystal structure of Ga^{III}−DOTA-D-PheNH$_2$. (b) Structural formula of NODAGA-Tyr^3-Octreotide.

The interest in peptide chelator conjugates for labeling with gallium radionuclides comes from their desirable physical properties (*17*, *18*). Three gallium radionuclides exist with decay characteristics that are suitable for γ-scintigraphy, PET imaging, and receptor-mediated radiotherapy: ^{68}Ga is a 68 min half-life-generator-produced positron emitter which is of interest because of the 280 d half-life of the parent ^{68}Ge. This gives the generator a long half-life of more than 1 year and allows PET imaging at institutions without on-site cyclotron.

^{67}Ga has a half-life of 78.3 h and decays via electron capture with 3 γ-emissions at 93 keV (38%), 185 keV (24%), and 300 keV (16%) which are useful for planar scintigraphy and single photon emission tomography (SPET). In addition, ^{67}Ga is also a reasonably efficient Auger-emitter for use in internal radiotherapy if the vectors used to bring the radionuclide to the tumor cell are being internalized and the radionuclide comes close to the nucleus.

^{66}Ga again is a positron emitter with an attractive intermediate half-life of 9.5 h which is of current interest because of its longer half-life, more suitable to the pharmacokinetics of a variety of biomolecules (*19*, *20*). It is cyclotron-produced and emits positrons with an abundance of 56% and E_{mean} = 1.7 MeV.

EXPERIMENTAL SECTION

Materials and Methods. *General Methods.* All chemicals were obtained from commercial sources and used

Scheme 1. Synthesis of NODAGA(tBu)$_3$ (6)

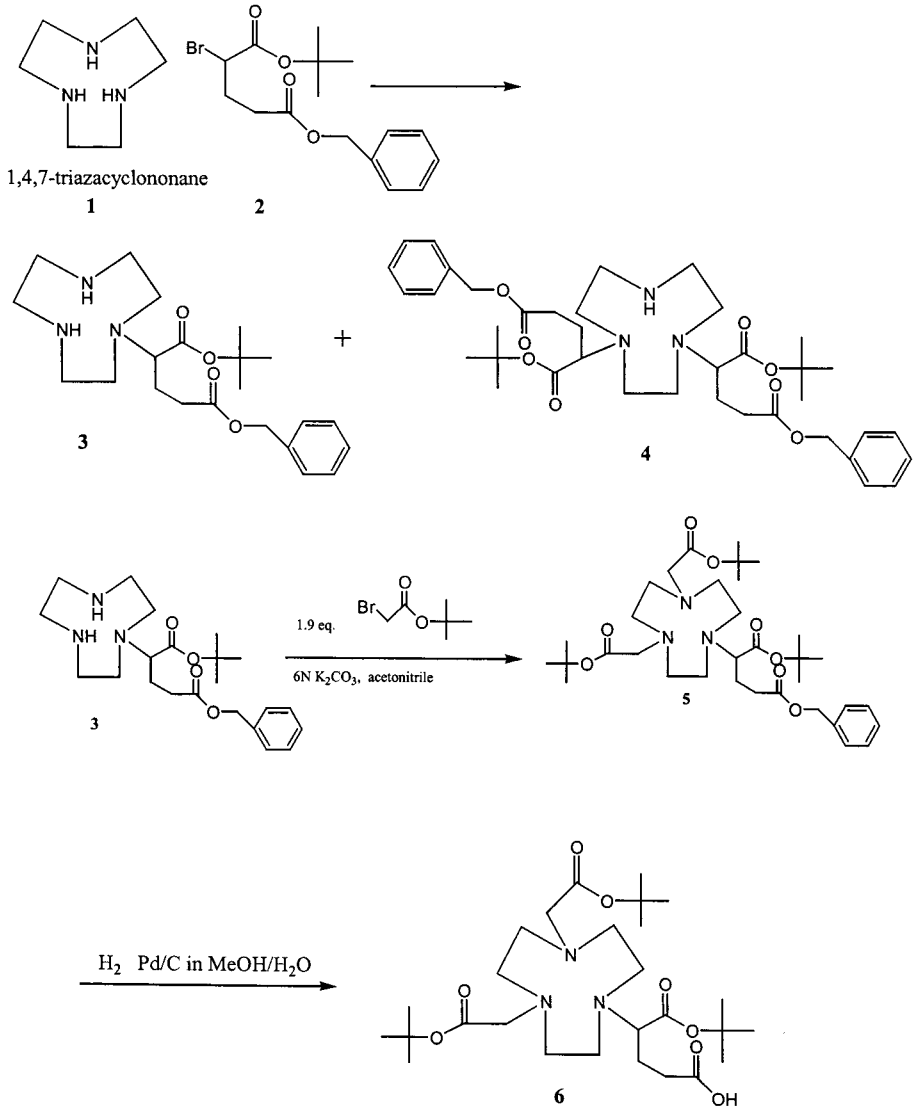

without further purification. 1,4,7-Triazacyclononane was commercially available (Macrocyclics, Dallas, TX). Octreotide was commercially available as Sandostatin (Novartis). [^{111}In]Cl_3 and [^{67}Ga]Cl_3 were purchased from Mallinckrodt Med. (Petten, The Netherlands). Chemical reactions were monitored by thin-layer chromatography (TLC) on Merck plates precoated with silica gel 60 F_{254} (0.25 mm). Spots were visualized either by UV light or iodine. Flash chromatography was performed on silica gel 60 (Fluka). Electrospray ionization (ESI) mass spectroscopy was carried out with a Finnigan SSQ 7000 spectrometer or fast atom bombardment (FAB) mass spectroscopy with a VG 70SE spectrometer. Analytical and semipreparative HPLC was performed on a Hewlett-Packard 1050 HPLC system with a multiwavelength detector and a flow-through Berthold LB 506 Cl γ-detector with a Macherey-Nagel Nucleosil 120 C_{18} column and preparative HPLC on a Metrohm HPLC system LC−CaDI 22−14 with a Macherey-Nagel VP 250/21 Nucleosil 100−5 C_{18} column. Quantitative γ-counting was performed on a COBRA 5003 γ-system well counter from Packard Instrument. ^{1}H and ^{13}C NMR was performed with either a Brucker spectrometer at 360/99 MHz or a Varian VXR 400 at 400/101 MHz. Chemical shifts reported are relative to trimethylsilane (TMS). Solid-phase peptide synthesis was performed on a semiautomatic peptide synthesizer commercially available from Rink Combichem (Bubendorf, Switzerland). The cell culture medium was Dulbecco's minimal essential medium (DMEM) from GibcoBRL. DOTA-Tyr^3-octreotide (DOTATOC) was synthesized as described before (*11*).

Synthesis. Starting from the commercially available glutamic acid 5-benzyl ester, α-bromoglutaric acid diester (**2**) (Scheme 1) was synthesized in two steps as described before (*21*).

1-(1-Carbobenzyloxy-3-carbo-*tert*-butoxypropyl)-1,4,7-triazacyclononane (3). A solution of 513 mg (1.44 mmol) of α-bromoglutaric acid 1-*tert*-butyl ester 5-benzyl ester (**2**) in 20 mL of chloroform was added over a period of 3 h to a solution of 557 mg (4.31 mmol) of 1,4,7 triazacyclononane in 20 mL of chloroform. The mixture was stirred over 3 d at room temperature and concentrated to a brown oil. The crude product was purified by column chromatography with silica gel 60 (5 × 20 cm; eluents: 250 mL of ethanol/ammonia 95:5; 300 mL of chloroform/ethanol/ammonia 7:3:0.5). Yield: 404 mg (69.2%) of a colorless oil. Unreacted 1,4,7-triazacyclononane was recovered and can be reused after distillation. ^{1}H NMR [$CDCl_3$, RT]: δ 1.5 (s, 9H, C(CH_3)$_3$); 2.2−1.85 (m, 2H, CHNCH_2); 2.9−2.5 (m, 14H, NCH_2, CH_2COOBzl); 3.25 (dd, 1H, C*H*Br); 5.1 (s, 2H, CH_2Ph); 7.35 (m, 5H, arom); ^{13}C NMR [$CDCl_3$, RT]: δ 24.7, 25.2 (CH_2CHN);

28.1 (C(CH_3)$_3$); 31.0 (CH_2COOBzl); 46.5, 46.6, 49.8 (NCH_2); 65.4, 65.7 (HCNCH_2); 66.1 (COOCH_2Phe); 81.0 (C(CH$_3$)$_3$); 126.6, 126.9, 128.1, 128.2, 128.4 (arom); 135.8 (arom) 172.0, 172.7, 173.0 (*C*OOtBu, *C*OOBzl); IR (KBr, cm^{-1}): 2931 (ν as, CH_2); 2850 (ν sym, CH_2); 1725 (ν as C=O, COOtBu, COOBzl); 1368 (δ C(CH_3)$_3$); 1152 (ν C−O); 753, 699 (arom). EI-MS (*m*/*z* (%)): 406.1 (46, [M + H]$^+$); 350.1 (100, [M − C_4H_9]$^+$).

Analytical data of the side product 1,4-(1-carbobenzyloxy-3-carbo-*tert*-butoxypropyl)-1,4,7-triazacyclononane (**4**): ^{1}H NMR [$CDCl_3$, RT]: δ 1.0 (s, 18H, C(CH_3)$_3$); 1.35−1.7 (m, 4H, CHNCH_2); 1.9−2.45, 2.6−2.8 (2m, 16H, NCH_2, CH_2COOBzl); 3.2 (m, 2H, C*H*Br); 4.6 (s, 4H, CH_2Ph); 6.8 (m, 10H, arom); EI-MS, *m*/*z* (relative intensity): 682.3 (100, [M + H]$^+$); 626.2 (15, [M − C_4H_9]$^+$); 570.1 (10, [M − 2C_4H_9]$^+$).

1-(1-Carbobenzyloxy-3-carbo-*tert*-butoxypropyl)-4,7-bis(carbo-*tert*-butoxymethyl)-1,4,7-triazacyclononane (5). A 390 mg (0.963 mmol) amount of [1-(1-carbobenzyloxy-3-carbo-*tert*-butoxypropyl)-1,4,7-triazacyclononane] (**3**) in 30 mL of dry acetonitrile is cooled to 4 °C. A 255 μL (1.733 mmol) amount *tert*-butylbromoacetic acid was added dropwise over a period of 15 min. The reaction mixture was stirred for additional 15 min before adding 728 mg (5.271 mmol) of dry potassium carbonate and allowed to warm slowly to room temperature over 4 h. The mixture was filtered afterward over Celite and evaporated to dryness to afford the crude product (540 mg, 95%) which can be used for the next step without further purification. Purification was also done by silica gel chromatography (5 × 20 cm; eluents: 80 mL of ethyl acetate; 100 mL of $CHCl_3$/EtOH 20:1; 100 mL of $CHCl_3$/EtOH 4:1). ^{1}H NMR [$CDCl_3$, RT]: δ 1.5 (s, 27H, C(CH_3)$_3$); 1.85−3.6 (m, 21H, C*H*NCH_2, NCH_2, CH_2-COOBzl, CH_2COOtBu); 5.1 (s, 2H, CH_2Ph); 7.35 (m, 5H, arom); ^{13}C NMR [$CDCl_3$, RT]: δ 24.7, 25.3 (*C*H_2CHN); 27.3, 27.7, 28.1, 28.3 (C(*C*H$_3$)$_3$); 30.9, 31.0, 31.3 (*C*H_2-COOBzl, *C*H_2COOtBu)); 50.5, 51.5, 53.1, 58.2 (N*C*H_2); 65.4 (H*C*NCH_2); 66.4 (COO*C*H_2Phe); 81.3, 81.7, 82.1 (*C*(CH$_3$)$_3$); 127.0, 127.5, 128.2, 128.3, 128.7 (arom); 136.0 (arom) 170.7, 171.4, 172.1, 172.8, 173.1 (*C*OOtBu, *C*OOBzl); IR (KBr, cm^{-1}): ν = 2975, 2927 (ν as, CH_2); 2854 (ν sym, CH_2); 1734 (ν as C=O, COOtBu, COOBzl); 1368 (δ C(CH_3)$_3$); 1153 (ν C−O); 753, 699 (arom). EI-MS, *m*/*z* (relative intensity): 635, 634 (100, [M + H]$^+$).

1-(1-Carboxy-3-carbo-*tert*-butoxypropyl)-4,7-(carbo-*tert*-butoxymethyl)-1,4,7-triazacyclononane (NODAGA(tBu)$_3$) (6). A 150 mg (0.237 mmol) of 1-(1-carbobenzyloxy-3-carbo-*tert*-butoxypropyl)-4,7-(carbo-*tert*-butoxymethyl)-1,4,7-triazacyclononane (**5**) was dissolved in 20 mL of 2-propanol and 50 mg 10% Pd/C suspended in 0.5 mL of H_2O was added. The mixture was treated by bubbling hydrogen through the solution over 18 h, filtered over Celite, and evaporated to dryness. The residue was chromatographed on silica gel 60 (2-propanol/ammonia 95:5) to obtain 85 mg (66%) of a yellow oil. ^{1}H NMR [$CDCl_3$, RT]: δ 1.5 (s, 27H, C(CH_3)$_3$); 2.0 (m, 2H, CH_2COOH); 2.5 (m, 2H, NCHCH_2); 2.8−3.2 (m, 12H, NCH_2); 3.45−3.75 (m, 5H, C*H*NCH_2, CH_2COOtBu); ^{13}C NMR [$CDCl_3$, RT]: δ 25.1, 25.2 (*C*H_2CHN); 27.8, 28.0 (C(*C*H$_3$)$_3$); 32.7 (*C*H_2COOH, *C*H_2COOtBu)); 49.3, 51.7, 52.6, 57.2 (N*C*H_2); 65.5 (H*C*NCH_2); 81.1, 82.0 (*C*(CH$_3$)$_3$); 169.4, 171.1 (*C*OOtBu); 176.5 (*C*OOH); IR (KBr, cm^{-1}): ν = 2977, 2932 (ν as, CH_2); 1727 (ν as C=O, COOtBu, COOH); 1368 (δ C(CH_3)$_3$); 1251 (ν C−OH); 1156 (ν C−O). EI-MS, *m*/*z* (relative intensity): 1088 (10, [2M + H]$^{2+}$); 567, 566 (12, [M + Na]$^+$); 545, 544 (100, [M + H]$^+$).

Synthesis of NODAGATOC (8). D-Phe^1-Cys(Acm)^2-Tyr(tBu)^3-D-Trp(Boc)^4-Lys(Boc)^5-Thr(tBu)^6-Cys(Acm)^7-Thr(tBu)^8-ol (**7**) was assembled on a trityl chloride resin (TCP, Pepchem, Tübingen, Germany) using standard Fmoc (9-fluorenylmethoxycarbonyl) strategy (*22*) with diisopropylcarbodiimide (DIC) as coupling reagent. The coupling of the chelator was done as follows: 81 mg of octapeptide (18.3 μmol peptide, 0.9 mmol/g resin) assembled on TCP-resin was incubated for 4 h with a mixture of a 40 min preincubated solution of 30 mg (0.055 mmol) (**6**) and 21 mg (0.055 mmol) of HATU (*O*-(7-azabenzotriazol-1-yl)-*N*,*N*,*N*',*N*'-tetramethyluronium-hexafluoro-phosphate) in 2 mL of NMP (*N*-methylpyrrolidone). The pH was adjusted to 7−8 using DIPEA (diisopropylethylamine, 10 μL, 0.06 mmol). The peptide was cleaved from the resin with 20% acetic acid in dichloromethane (five times 3 mL) and coevaporated three times with toluene (100 mL) to remove the acetic acid. Then it was cyclized with 10 equiv of iodine in methanol/water 9:1, deprotected with TFA/phenol/thioanisole/water 85:5:5:5 for 4−6 h, and purified by preparative HPLC (Macherey-Nagel Nucleosil 100−5 C_{18}, flow: 15 mL/min; eluents: A = 0.1% trifluoroacetic acid (TFA) in water and B = acetonitrile; nonlinear gradient: 0 min, 85% A; 20 min, 70% A). MS ((−)EI, *m*/*z* (%)): 1391.1 (100, [M − H]$^-$); ((+)EI, *m*/*z* (%)): 1392.9 (8, [M + H]$^+$), 697.3 (100, [M + 2H]$^{2+}$). The overall yield based on the first Fmoc cleavage is 31.5%.

Ga−NODAGATOC (9). The ^{69,71}Ga^{III} complex was synthesized according to the methods previously described (*11*, *16*). A mixture of 500 μg (0.34 μmol) (**8**) in 500 μL of 0.4 M sodium acetate buffer (pH 5) was incubated with 102 μL of a 0.01 M aqueous solution of Ga(III) nitrate nonahydrate (1.02 μmol) for 25 min at 95 °C, cooled to room temperature, and purified over a SepPak C_{18} cartridge preconditioned with 10 mL of ethanol and 10 mL of water. The cartridge was eluted with 10 mL of 0.4 M sodium acetate (pH 5) followed by 3 mL of methanol resulting in 400 μg (76%) of Ga−NODAGATOC after evaporation of the methanol. MS ((−)EI, *m*/*z* (%)): 1495 (12, [M − H]$^-$); ((+)EI, *m*/*z* (%)): 1461 (14, [M + H]$^+$), 742 (100, [M + 2H]$^{2+}$).

In−NODAGATOC (10) was synthesized as (**9**) using $InCl_3$·5H_2O.

Radiotracer for Internalization Experiments. [^{111}In]−NODAGATOC was prepared by dissolving 10 μg of NODAGATOC (7.2 nmol) in sodium acetate buffer (100 μL, 0.4 M, pH 5); after the addition of $^{111}InCl_3$ (3.5 mCi), the solution was heated at 95° for 25 min. A 1.5 molar excess of $InCl_3$·5H_2O was added and the final solution heated at 95 °C for 25 min. [^{67}Ga]−NODAGATOC (10 μg of ligand, 3 mCi of $^{67}GaCl_3$) was prepared in the same way, using Ga(III) nitrate nonahydrate. In a modification of this protocol, acetate buffer was replaced by HEPES (150 μL, 0.1 M, pH 5.8). The final labeling solution had a pH 2.5. This protocol gave yields >95% at a specific activity of 40 GBq/μmol^{-1}. Subsequently radiolabeled peptides were purified utilizing a SepPak C_{18} cartridge preconditioned with 10 mL of methanol and 10 mL of water; the cartridge was eluted with 3 mL of water, followed by 2 mL of ethanol, to afford the very pure radioligand with a specific activity ≥15 GBq μmol^{-1}. A quality control was performed by HPLC (eluents: A = 0.1% TFA in water and B = acetonitrile; gradient: 0−30 min, 55% A, 30−36 min, 100% B, 36−40 min, 95% A).

Metal/Ligand Stability Studies. The chemical stability of the radiometal complexes [^{67}Ga]− and [^{111}In]−NODAGATOC was studied by measuring the rate of exchange of the radiometal in the presence of 10^5 molar excess of DTPA at pH 5. Solutions were stored at 37 °C,

and at periods up to 10 days aliquots were removed and analyzed by HPLC using the gradient described above.

Serum Stability. To 3 mL of fresh human serum, previously equilibrated in a 5% CO_2 (95% air) environment at 37 °C, was added 5 μCi of the [^{67}Ga]−NODAGATOC standard solution. The mixture was incubated in a 5% CO_2, 37 °C environment. At appropriate periods of time (0, 30 min, 1, and 4 h), 100 μL aliquots (in triplicate) were removed and treated with 200 μL of ethanol. Samples were then cooled (4 °C) and centrifuged for 15 min at 500*g* and 4 °C to precipitate serum proteins. One hundred microliters of supernatant was removed for activity counting in a γ well-counter. The sediment was washed twice with 1 mL of ethanol and counted. The activity in supernatant was compared with the activity in the pellet to give the percent peptide not bound to proteins.

The peptide structure in the supernatant was checked by HPLC using the equipment mentioned above.

Receptor Autoradiography and Binding Affinity. Determination of peptide conjugate concentrations and receptor autoradiography was described previously (*16*). Concentrations of peptides were determined spectrophotometrically using $\epsilon_{280} = 6800\ M^{-1}\ cm^{-1}$. IC_{50} values using autoradiographic methods were determined as described (*16*).

In brief, cells stably transfected with sst1-sst5 were kindly provided by Drs. T. Reisine and G. Singh (University of Pennsylvania, Philadelphia, PA). They were washed twice with and scraped into ice-cold 0.05 M Tris-HCl (pH 7.4), collected by centrifugation, and homogenized using a rotor/strator slash system (Polytron, Kinematica Inc., Littau, Switzerland) in the same buffer. After centrifugation at 120 g for 5 min at 4 °C, the supernatant was collected and centrifuged again at 48.000 g for 30 min at 4 °C. The resulting pellet was resuspended in ice-cold Tris buffer, transferred into a microfuge tube, and centrifuged at 20.000 g for 15 min at 4 °C. After withdrawal of the supernatant, the membrane pellet was stored at −80 °C.

Receptor autoradiography was performed on 20-μm-thick cryostat (Leitz 1720, Rockleigh, NJ) sections of the membrane pellets, mounted on microscope slides and then stored at −20 °C. For each of the tested compounds, complete displacement experiments were performed with the universal somatostatin radioligand [^{125}I]-[Leu^{8},D-Trp^{22},Trp^{25}]somatostatin 28 using increasing concentrations of the unlabeled peptide ranging from 0.1 to 1000 nM. As a control, somatostatin 28 was run in parallel using the same increasing concentrations. IC_{50} values were calculated after quantification of the data using a computer-assisted image processing system as described previously (*23*). Tissue standards (autoradiographic [^{125}I]-microscales, Amersham), containing known amounts of isotopes, cross-calibrated to tissue-equivalent ligand concentrations, were used for quantification (*24*).

Radiotracers Used in Biodistribution Studies. [^{67}Ga]−NODAGATOC and [^{111}In]−DOTATOC were prepared with the methodology described in the previous section, without addition of cold metal but using lower peptide amounts. If necessary, radioligands were purified by SepPak C_{18} cartridge and after evaporation of ethanol were diluted in NaCl (0.1% BSA, pH 7.4) to afford the very pure radioligands with a specific activity of ca. 40 GBq/μmol conjugate. The radiotracers were subjected to quality control by HPLC as described above.

Cell Culture. AR4-2J (ATCC, Manassas, VA) rat pancreatic tumor cells were cultured in Dulbecco's minimal essential medium (DMEM). DMEM was supplemented with vitamins, essential and nonessential amino acids, L-glutamine, antibiotics (peniciline/streptomycine), fungicide (amprotencine), and 10% fetal calf serum (FCS) as described elsewhere (*25*).

Internalization/Externalization Studies. Internalization and externalization experiments were performed as indicated in previous publications in six-well plates (*25, 26*). Briefly, the cells were washed twice with internalization medium [DMEM supplemented with 0.1% FCS, vitamins, essential and nonessential amino acids, L-glutamine, antibiotic (penicillin/streptomycin), and fungicide (amprotencin)], and they were allowed to adjust to the medium for 1 h at 37 °C. Approximately 3.7 kBq (2.5 pmol) of radioligand were added to the medium, and the cells, 10^6 cells per well, were incubated (in triplicates) for 4 h at 37 °C, 5% CO_2, with or without excess cold octreotide (300 μL of a 1 μM solution) to determine nonspecific internalization. The final volume was 3 mL. At appropriate time periods, the internalization was stopped by removal of the medium and washing the cells with ice-cold phosphate-buffered saline. Cells were then treated with glycine buffer twice for 5 min at room temperature (0.05 M glycine solution, pH adjusted to 2.8 with 1 N HCl) to distinguish between cell surface-bound (acid releasable) and internalized (acid resistant) radioligand. Finally, cells were treated with 1 N NaOH and incubated at 37 °C for 10 min to detach them from plates, and the radioactivity was measured in a γ-counter. For externalization the AR4-2J cells were allowed to internalize the radioligands for periods of 2 and 4 h and then were exposed to an acid wash, as described in the previous section, to dissociate cell-surface-receptor-bound radioligand. Three milliliters of culture medium were added to each well, cells were incubated at 37 °C in a 5% CO_2 environment, and externalization of the cell-incorporated radioactivity was studied during 3 h.

Biodistribution Experiments in AR4-2J Tumor-Bearing Nude Mice. Six to ten week old Swiss female nude mice (IFFA-CREDO, France) were implanted subcutaneously with 5 million AR4-2J rat pancreatic tumor cells, previously expanded in Dulbecco's minimal essential medium (DMEM, GibcoBRL). DMEM was supplemented with vitamins, essential and nonessential amino acids, L-glutamine, antibiotics (penicilline/streptomycine), fungicide (amprotencine), and 10% fetal calf serum (FCS).

Fourteen days after inoculation, the tumors weighed 50−100 mg, and the mice were injected in the lateral tail vein with 5 μCi of [^{67}Ga]−NODAGATOC or [^{111}In]−DOTATOC, diluted in NaCl (0.1% BSA, pH 7.4, total injected volume = 200 μL). For determination of nonspecific uptake in tumor or receptor-positive organs, a group of four animals was injected in the tail vein with 50 μg of cold octreotide in NaCl (injected volume, 200 μL), 30 min before radiotracer injection. At 4, 24, and 48 h mice (in groups of three or four) were sacrificed and organs of interest collected, rinsed of excess blood, weighed, and counted in a γ-counter. The percentage of injected dose per gram (% ID/g) was calculated for each tissue. The total counts injected per animal were determined by extrapolation from counts of an aliquot taken from the injected solution. Urine samples were analyzed for possible metabolites by HPLC.

All animal experiments were performed in compliance with the Swiss regulation for animal treatment (Bundesamt für Veterinärwesen, approval no. 789).

RESULTS

Synthesis and Radiolabeling. An important step toward the synthesis of NOTA-derivatized bioactive

Scheme 2. Synthesis of NODAGATOC (8)

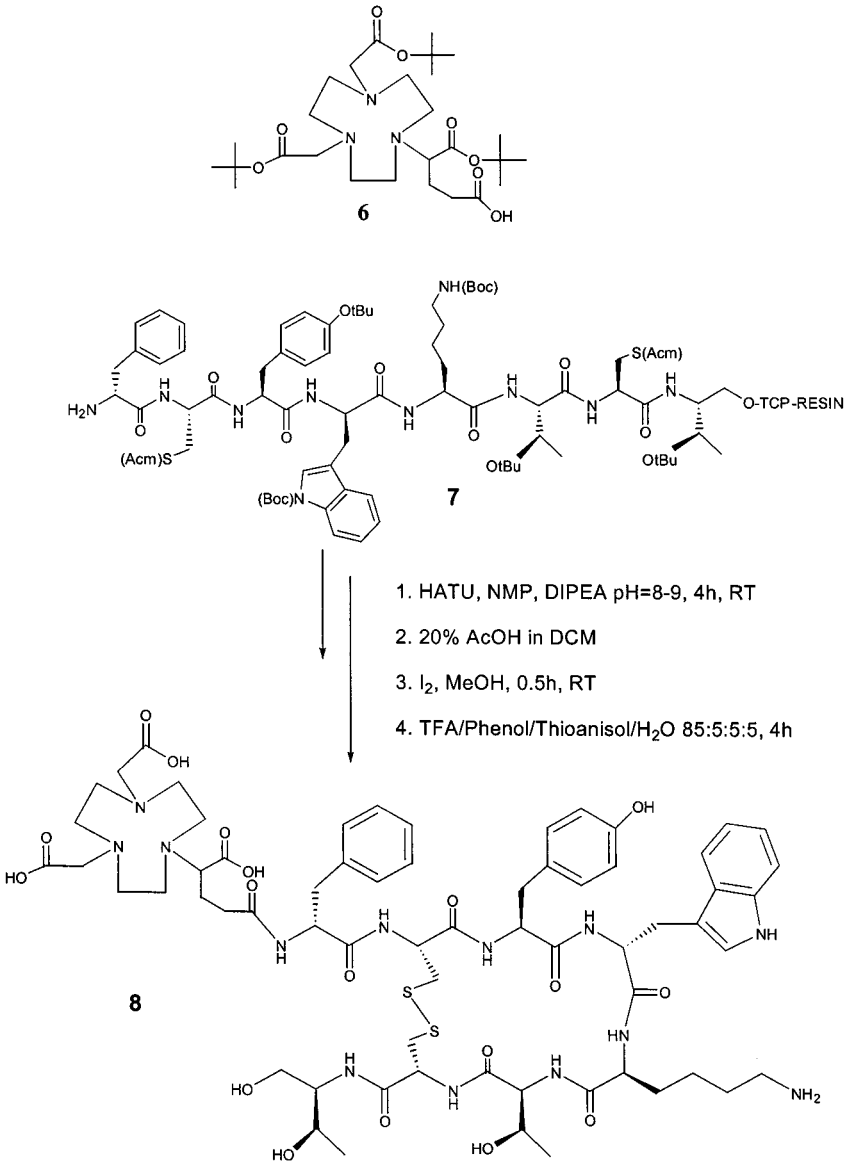

Table 1. Yields of the Monoalkylation of 1,4,7-Triazacyclononane (1) with *β*-Bromoglutaric Acid 1-*tert*-Butyl Ester 5-Benzyl Ester (2)

ratio of **1** to **2**	% yield of monoalkylated product	% yield of dialkylated product
1.3:1	36.9	23
2:1	50.9	20
3:1	69.2	>5

peptides is the development of the corresponding prochelator NODAGA(tBu)$_3$ (**6**) (Scheme 1). The monoreactive NODAGA-prochelator was synthesized in five steps with an overall yield of 21% (Schemes 1 and 2). Two side reactions decreased the yields of steps 3 and 4. The monoalkylation of 1,4,7-triazacyclononane (**1**) with α-bromoglutaric acid 1-*tert*-butyl ester 5-benzyl ester (**2**) gave more than 20% of the dialkylated product 1,4-bis(1-carbobenzyloxy-3-carbo-*tert*-butoxypropyl)-1,4,7-triazacyclononane (**3a**) if the ratio of **1**:**2** was 2. Only the use of a 3-fold excess of **1** over **2** gave yields based on **2** of about 70% (Table 1). In step 4, overalkylation to a quarternary ammonium salt was found even if stoichiometric ratios were used. Therefore only 1.9 equiv of bromoacetic acid *tert*-butyl ester were employed. In addition, cooling to 4 °C appeared to be advantageous to avoid overalkylation.

After these partially optimized synthetic steps, **6** was obtained in a reasonable overall yield of 21%. The linear side chain protected octapeptide D-Phe^1-Cys(Acm)^2-Tyr-(tBu)^3-D-Trp(Boc)^4-Lys(Boc)^5-Thr(tBu)^6-Cys(Acm)^7-Thr-(ol)(tBu)^8 **(7)** was assembled on a TCP resin using Fmoc-strategy (*22*) with DIC as coupling reagent. **6** (3 equiv) was coupled to **7** on the resin with the use of HATU (*O*-(7-azabenzotriazol-1-yl)-*N*,*N*,*N*',*N*'-tetramethyluronium hexafluorophosphate) as coupling reagent. The protected peptide was mildly cleaved from the resin (20% CH_3-COOH), cyclized with I_2 in methanol, deprotected, and purified by preparative HPLC analogous to Arano et al. (*27*) (Scheme 2). Reversed phase HPLC afforded the peptide in ≥95% purity. The composition and structure of NODAGATOC were verified by MS-ESI and by the retention of a high-binding affinity to sstr2. NODAGATOC was labeled with the radiometals of interest (^{67}Ga, ^{111}In) using acetate buffer (pH 5, 0.4 M) by heating (95 °C, 25−30 min); the labeling yields were >99% (^{111}In) and >60% (^{67}Ga) at a specific activity >40 GBq μmol^{-1}. It could be shown by an accidental labeling protocol that using HEPES (pH ≈ 2.5) better labeling yields (≥95% at 40 GBq μmol^{-1}) of [^{67}Ga]NODAGATOC were obtained. We assume that this is due to the lower pH which may

Table 2. Affinity Profiles (IC_{50}) for Human sst1−sst5 Receptors of a Series of Somatostatin Analogues. IC_{50} Values (nM ± SE) Are in Triplicates. Number of Independent Studies in Brackets. Somatostatin-28 Is Used as Internal Control in Each of the Experiments

peptide	hsst1	hsst2	hsst3	hsst4	hsst5
somatostatin-28	4.1 ± 0.3 (15)	2.6 ± 0.2 (16)	5.4 ± 0.6 (13)	4.1 ± 0.3 (16)	3.9 ± 0.4 (17)
DOTA-Tyr^3-octreotide (DOTATOC)	>10000 (7)	13.9 ± 2.8 (6)	816 ± 259 (5)	>1000 (5)	393 ± 85 (6)
Y-DOTA-Tyr^3-octreotide[a]	>10000 (6)	11.4 ± 1.7 (6)	389 ± 135 (5)	>10000 (6)	204 ± 92 (6)
Ga-DOTA-Tyr^3-octreotide	>10000 (6)	2.5 ± 0.5 (7)	607 ± 165 (6)	>1000 (6)	106 ± 37 (7)
NODAGA-Tyr^3-octreotide (NODAGATOC)	>10000 (2)	3.2 ± 1.0 (2)	675 ± 225 (2)	>1000 (2)	305 ± 85 (2)
Ga−NODAGA-Tyr^3-octreotide	>1000 (2)	3.5 ± 1.6 (2)	325 ± 55 (2)	>1000 (2)	185 ± 35 (2)
In−NODAGA-Tyr^3-octreotide	>1000 (3)	1.7 ± 0.2 (3)	293 ± 71 (3)	320 ± 17 (3)	44 ± 8 (3)

[a] In−DOTA-Tyr^3-octreotide was shown to have the same sstr2 receptor affinity as Y^{III}−DOTA-Tyr^3-octreotide using a somewhat different assay *(11)*.

favor the $^{67}Ga^{3+}$ over the metal impurities present. An expansion of this finding was outside the scope of this work.

Receptor Binding. Table 2 shows the newly synthesized NODAGATOC somatostatin analogues investigated and their respective IC_{50} values for the five somatostatin receptor subtypes. As controls, somatostatin 28 (SS28), which binds with high affinity to all five somatostatin receptor subtypes, and our gold standards Ga/Y-DOTATOC were included. Ga−NODAGATOC shows high affinity only to sstr2 with an IC_{50} of 3.5 ± 1.6 nM close to the one of Ga-DOTATOC (2.5 ± 0.5 nM) whereas it binds significantly better to sstr2 than Y-/In-DOTATOC. Measurable affinity was also found to sstr3 and sstr5. Interestingly, In−NODAGATOC binds with higher affinity to sstr2 (1.7 ± 0.2 nM) and also has distinctly higher affinity to sstr4/sstr5 than Ga−NODAGATOC. A remarkably low IC_{50} value was found for sstr5, and no binding affinity was found to sstr1.

Stability of the Radiotracers. Our studies had demonstrated that with both radiolabeled peptides no radiolysis breakdown products were observed and that there is no appreciable release of ^{67}Ga even under extreme conditions (10^5 times excess of DTPA). The pseudo first-order dissociation rate constant for [^{67}Ga]−NODAGATOC was shown to be $<10^{-8}$ s^{-1} compared to 3.5×10^{-6} s^{-1} for [^{111}In]−NODAGATOC.

Stability in Serum. Incubation of [^{67}Ga]−NODAGATOC in fresh human serum shows high metabolic stability as well as high stability with regard to transchelation. At 4 h, 98.3% of the activity remained in the nonproteic fraction. We found also, by HPLC, that the radioactivity present in this fraction, after 4 h of incubation, was still peptide bound and represents intact radioligand indicating that no transchelation or appreciable metabolic decay did take place.

Stability in Rat Liver Homogenate. The possible degradation of [^{67}Ga]−NODAGA-Tyr^3-octreotide was studied in 30% rat liver homogenate, a medium rich in peptidases and proteinases. The analysis was carried out by HPLC and until 4 h of incubation no degradation products were observed.

[^{67}Ga]/[^{111}In]−NODAGATOC Internalization and Externalization Results. The AR4-2J rat pancreatic carcinoma cell line is known to express sstr2 receptors both in vivo and in vitro (*28*). The two radioligands were internalized by AR4-2J cells in a time dependent way, as shown in Figure 2. Both radiopeptides showed a fast and time dependent cell uptake by endocytosis which did not reach a plateau within 4 h of incubation at 37 °C. There was no difference between the two radioligands. Both show about 18% (of the added activity) specific internalization after 2 h compared to only about 6% of [^{111}In]−DOTATOC (Figure 3). Internalization was strongly reduced in the presence of 0.1 μM unlabeled octreotide

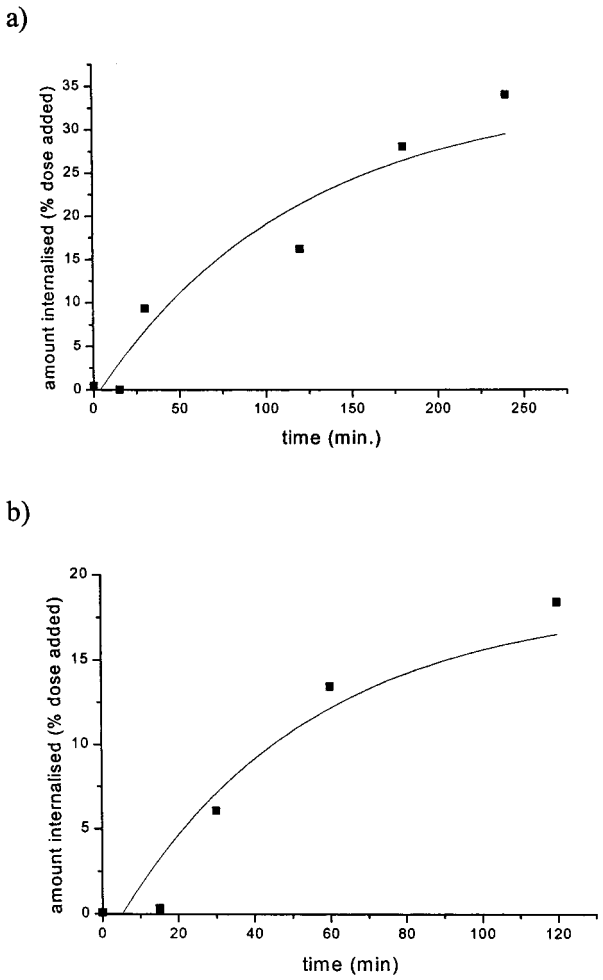

Figure 2. Uptake kinetics on rat pancreatic tumor AR4-2J cells of (a) [^{111}In]−NODAGA-Tyr^3-octreotide and (b) [^{67}Ga]−NODAGA-Tyr^3-octreotide. Data result from two independent experiments with triplicates in each experiment.

(data not shown). In fact, nonspecific internalization was <3% of the added activity. The surface bound peptide (acid removable) was <7% of the added activity. The externalization of both peptides was studied with cells exposed 2 and/or 4 h to the radioligand as described for internalization (Figure 4). Again a time dependent externalization was found which appears to depend somewhat on the time period cells were allowed to internalize as well as on the radioligand studied. Interestingly, the externalized radiopeptides were shown to be intact by HPLC as they coelute with the original radiopeptides.

Animal Biodistribution Studies. Biodistribution data were obtained by comparing [^{67}Ga]−NODAGATOC with our gold standard for sstr2 receptor targeting [^{111}In]−DOTATOC. The biodistribution of the latter was

Table 3. Biodistribution and Tissue Ratios in AR4-2J Tumor-Bearing Nude Mice. Results Are the Mean of Groups of Three or Four Animals

site	[^{67}Ga]−NODAGATOC (4 h)		[^{111}In]−DOTATOC (4 h)		[^{67}Ga]−NODAGATOC (24 h)[b]	[^{111}In]−DOTATOC (24 h)[b]	[^{67}Ga]−NODAGATOC (48 h)[b]
	unblocked	blocked[a]	unblocked	blocked[a]			
	Biodistribution (%ID/g for three or four animals)						
blood	0.05 ± 0.004	0.04 ± 0.01	0.07 ± 0.04	0.06 ± 0.009	0.007 ± 0.0009	0.008 ± 0.002	0.003 ± 0.0005
pancreas	1.25 ± 0.67	0.26 ± 0.06	1.10 ± 0.15	0.14 ± 0.11	0.22 ± 0.26	0.35 ± 0.10	0.02 ± 0.005
s. intest.	0.70 ± 0.08	0.14 ± 0.05	0.29 ± 0.06	0.09 ± 0.03	0.07 ± 0.02	0.07 ± 0.01	0.02 ± 0.006
spleen	0.19 ± 0.04	0.06 ± 0.02	0.16 ± 0.03	0.10 ± 0.02	0.03 ± 0.008	0.08 ± 0.03	0.02 ± 0.005
liver	0.16 ± 0.02	0.18 ± 0.05	0.23 ± 0.04	0.27 ± 0.04	0.02 ± 0.0002	0.09 ± 0.009	0.01 ± 0.003
stomach	4.80 ± 0.67	0.56 ± 0.08	2.77 ± 0.73	0.41 ± 0.35	0.38 ± 0.06	0.78 ± 0.08	0.11 ± 0.01
adrenals	2.90 ± 0.43	0.70 ± 0.17	1.46 ± 0.13	0.35 ± 0.21	0.46 ± 0.13	0.53 ± 0.07	0.42 ± 0.26
kidney	7.08 ± 1.50	18.0 ± 2.95	12.84 ± 0.98	12.55 ± 1.30	0.46 ± 0.05	5.64 ± 0.66	0.22 ± 0.04
lung	0.46 ± 0.03	0.19 ± 0.05	0.28 ± 0.07	0.16 ± 0.03	0.09 ± 0.09	0.12 ± 0.01	0.05 ± 0.07
heart	0.08 ± 0.01	0.05 ± 0.01	0.07 ± 0.02	0.05 ± 0.008	0.02 ± 0.003	0.03 ± 0.003	0.01± 0.003
tumor	21.21 ± 3.55	3.64 ± 1.39	12.50 ± 0.65	6.81 ± 0.03	2.60 ± 0.47	5.60 ± 0.48	0.73 ± 0.20
	Tissue Ratio						
tumor/blood	424		188		321	700	243
tumor/liver	133		54		130	62	37
tumor/kidney	3		0.97		5.7	0.94	3.3

[a] Blocked with 50 μg of octreotide 30 min before injection of radiopeptide. [b] Unblocked.

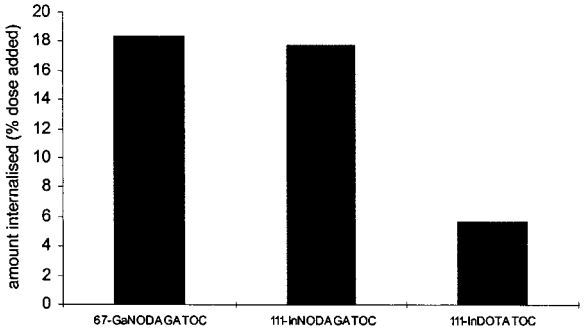

Figure 3. Uptake on rat pancreatic tumor AR4-2J cells of [^{67}-Ga]−NODAGA-Tyr^3-octreotide, [^{111}In]−NODAGA-Tyr^3-octreotide, and [^{111}In]−DOTA-Tyr^3-octreotide, 2 h after incubation with ca. 0.09 μCi of the radiolabeled peptides in a 37 °C, 5% CO_2 environment.

reported before (*11*, *25*, *26*, *28*) and was used as a reference because a new batch of AR4-2J cells was used. Data obtained with nude mice bearing the AR4-2J pancreatic tumor are presented in Table 3 as % of injected dose per gram of tissue (% ID/g) as a function of time.

Both peptides displayed rapid blood clearance with only 0.05−0.07% ID/g remaining in blood at 4 h which can be associated with a fast elimination of radioactivity from the sstr-negative tissues not involved in the excretion process. In accordance with previous results (*28*) using [^{111}In]−DOTATOC and [^{67}Ga]−DOTATOC, [^{67}Ga]−NODAGATOC is excreted mainly by the kidney pathway, leading to very low liver uptake. Moreover, our HPLC studies in mouse urine demonstrated that the [^{67}Ga]−NODAGATOC is excreted unchanged in the first 4 h after radiotracer injection. [^{67}Ga]−NODAGATOC shows high uptake values in sst receptor expressing organs such as adrenals, pancreas, and stomach, and in the AR4-2J tumor. In addition, a very rapid clearance from all other organs and tissues except the kidneys was found. The results of an in vivo competition experiment using large excess of octreotide preinjected iv resulted in a >83% reduction of tumor uptake and also in a reduction of the uptake in the sstr-positive organs (80% in pancreas, 82% in stomach, 76% in adrenals). The injection of the blocking dose had no significant influence on the uptake in nontarget organs except the kidneys where the uptake is increased by a factor of >2.

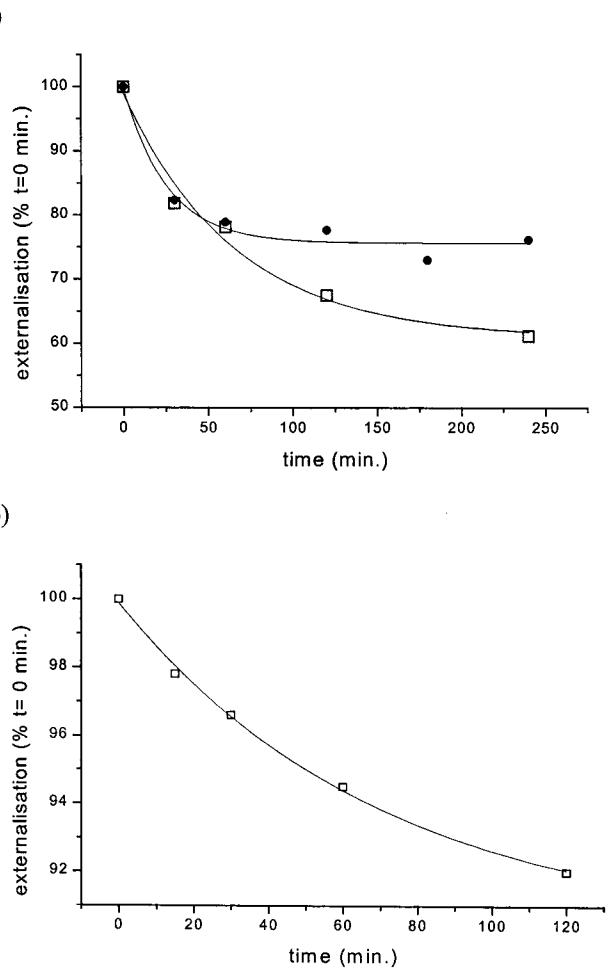

Figure 4. Externalization kinetics of (a) [^{111}In]−NODAGA-Tyr^3-octreotide and (b) [^{67}Ga]−NODAGA-Tyr^3-octreotide, by rat pancreatic AR4-2J tumor cells. Efflux of the radiolabeled peptides is expressed in percentage of radioactivity associated with the cells after acid wash retained in the cell compared with the uptake at 2 h (squares) or 4 h (circles) considered as 100%. After this period, the cells were exposed to an acid wash to remove cell surface bound radioligand. Each point represents two experiments carried out in triplicate.

[^{67}Ga]−NODAGATOC has a higher uptake in all sstr-positive tissues than [^{111}In]−DOTATOC at 4 h (tumor, 21.2 ± 3.5% ID/g vs 12.5 ± 0.65%; pancreas, 1.25 ± 0.67%

ID/g vs 1.1 ± 0.25; stomach, 4.8 ± 0.67% ID/g vs 2.77 ± 0.75% ID/g; adrenals, 2.9 ± 0.43% ID/g vs 1.46 ± 0.35% ID/g). A further remarkable result of the new radiopeptide is the very favorable tumor:kidney ratio which is 3.0 at 4 h compared to 1 for ^{111}In−DOTATOC, the ratio even increases at 24 h to 5.7 whereas it remains 1 at 24 h for ^{111}In−DOTATOC. Additional tumor/unspecific tissue ratios at 4 h can be seen from Table 3. They are as follows (in parentheses the data for ^{111}In−DOTATOC are given): 424 (188) for tumor/blood and 133 (54) for tumor/liver. These very favorable ratios indicate the high potential of this radiopeptide for early time point, highly sensitive diagnostic tumor imaging. An unexpected result is the relatively quick washout from the tumor and receptor-positive organs. In the tumor, the dose dropped from 21.2% ID/g at 4 h to 2.6% ID/g at 24 h and 0.73% ID/g at 48 h. A similar rate of decline is found in the other receptor-positive organs. Somewhat fortunately, this decline is even faster in the kidneys. The residence time of ^{111}In−DOTATOC is distinctly longer in receptor-positive tissues but also in the kidneys.

DISCUSSION

In the past few years several SRIF-derived positron-emitting radiopeptides have been developed (*12, 13, 29*−*32*), and some of them had been or are currently being investigated for PET imaging of SRIF receptor-positive tumors in patients (*33*−*35*). An ideal PET tracer will allow to answer many important questions in the new and rising field of tumor targeting with use of radiopeptides, e.g., receptor regulation due to pharmacologic and chemotherapeutic intervention, receptor quantification and potential receptor downregulation due to receptor mediated radiopeptide therapy. The radiopeptides discussed in this manuscript were designed to answer questions arising from earlier developments in our laboratory and to offer new conjugates for studies with the Ga^{III}, In^{III}, and Cu^{II} (*36*) radioisotopes. The macrocyclic chelator NOTA satisfies the coordination requirements of the respective metal ions in the indicated oxidation states. The NODAGATOC differs from our gold standard DOTA−[Tyr^3]-octreotide (DOTATOC) by the coupling of a new macrocyclic chelator to [tyr^3]-octreotide. We synthesized first a new bifunctional derivative of NOTA which had to fulfill two criteria:

(1) Compatibility with peptide synthesis; in other words, an orthogonally carboxylic acid group protected NOTA derivative has to be synthesized which upon specific deprotection of one carboxylic acid group is soluble in the common solvens used in solid-phase synthesis and may be used as an amino acid surrogate for coupling to the N-terminus of a requested peptide. (2) In addition, three acetate arms should be retained for metal coordination necessitating preparation of a C-functionalized NOTA. Different syntheses of bifunctional NOTA derivatives have been reported before by Parker et al. (overall yield: 7.7%) (*37*), Meares and Studer (yield: 1.34%) (*38*), and McMurray et al. (yield: 6.4%) (*36*). Their syntheses used intra- or intermolecular cyclization strategy as key steps affording NOTA's functionalized on a carbon of the macrocyclic ring. They were not designed for coupling to peptides, and harsh conditions for deprotection and reduction were necessary. Our aim was to introduce the carboxy function for coupling on the methylene group of a carboxymethyl arm, allowing one to start with commercially available triaazacyclononane, thus avoiding a cyclization step. A similar strategy was used by Brechbiel et al. (*39*) to yield a bifunctional NOTA for antibody modification in 9% overall yield. In addition, this strategy was used in the functionalization of DOTA (*21, 40*−*41*). The key steps are the synthesis of an orthogonally protected bromoalkyl dicarboxylic acid diester and the monoalkylation of the triazacyclononane macrocycle. The latter step was performed using 3 equiv of 1,4,7-triazacyclononane over the alkylating diester to give **3** (69.2%). **5** was obtained in 90% yield using somewhat less than 2 equiv of bromoacetic acid *tert*-butyl ester to avoid overalkylation. The overall yield of the five steps was about 21%. The coupling of **6** to the linear octapeptide (appropriately protected) assembled on the TCP-resin was straightforward. The cleavage was followed by oxidative cyclization using I_2 and deprotection in a mixture of TFA/phenol/thioanisole/water. The crude mixture was purified by preparative HPLC.

We have proposed earlier the use of a similar bifunctional chelator (NODASA = 1,4,7-triazacyclononane-1-succinic acid-4,7-diacetic acid) and the use of the radiogallium complex in a prelabeling approach (*42*). Although this approach is very attractive and was proven to work well with model peptides and with the nonradioactive Ga^{III}, it proved not to be practical for larger amounts of radioactivity because of relatively low coupling yields of [^{67}Ga]−NODASA to the peptide due to low solubility. This caused a large waste of radioactivity. The coupling of the present prochelator works well under peptide synthesis conditions and allows the preparation of a kit-formulated version of the conjugate.

Receptor Binding Studies. One of the aims of this study was to probe the hypothesis that the higher sstr2 affinity of [Ga^{III}]−DOTA-Tyr^3-octreotide vs [Y^{III}]−DOTA-Tyr^3-octreotide and [In^{III}]−DOTA-Tyr^3-octreotide can be explained by the different metal complex geometries of the respective metal DOTA-D-Phe coordination compounds which result in a spacer function between the Ga^{III} complex and the pharmacophoric peptide. This is due to the fact that the carboxyamido group connecting the two entities is not participating in the metal coordination contrary to the octadentate nature of the chelate unit in [Y^{III}]−DOTA-D-Phe. If this were true, [Ga^{III}]−NODAGATOC should have a receptor affinity closer to Ga^{III}−DOTATOC than [Y^{III}(In^{III})]DOTATOC. Indeed, we interpret the value of 3.5 ± 1.6 nM, which is very close to the value of [Ga^{III}]−DOTATOC, as originating from the structurally introduced ethylene spacer function. It is remarkable and not foreseen that [In^{III}]−NODAGATOC shows significant differences compared to [Ga^{III}]−NODAGATOC not only with regard to the sstr2 affinity which with 1.7 ± 0.2 nM is significantly higher than the one of [Ga^{III}]−NODAGATOC. Also, the affinity to sst4 and sst5 is significantly higher for the [In^{III}]−NODAGATOC vs [Ga^{III}]−NODAGATOC. The structural factors contributing to this difference are not clear. Both metals fit well into the cavity offered by NOTA. X-ray structural data point at potential differences. Whereas In^{III} (ionic radius = 0.80 Å, CN6; 0.92 Å, CN8) (*43*) prefers coordination number 7 or 8, the smaller Ga^{III} (ionic radius = 0.62 Å) is perfectly satisfied by hexadentate ligands and fits well into the cavity offered by NOTA and functionalized derivatives of it (*42, 44*). In this context, it is interesting to note that in the solid-state In^{III}−NOTA is crystallizing with one Cl^- ion in a pentagonal bipyramidal coordination environment (*44*). We propose as a possible explanation of the above-mentioned affinity differences that in the biological fluids used in our assays either Cl^- or H_2O are being coordinated to In^{III}.

Stability of Tracers. [^{67}Ga]−NODAGATOC and [^{111}In]−NODAGATOC proved to be more or less stable

with regard to radiometal transfer. The ^{67}Ga-labeled peptide is $>10^3$ times more stable than [^{111}In]−NODAGATOC which correlates well with the thermodynamic stability of most of the triaza complexes of these two metals (e.g., log *K* (GaNOTA) = 30.98, log *K* (InNOTA) = 25.9 (*45*). Also, the metabolic stability is very high in fresh human serum and surprisingly in a rat liver homogenate (data not shown).

Cell Uptake and Release. The internalization and release of the two new radiopeptides was studied in the AR4-2J cell line known to express sstr2 receptors (*28*). The cell uptake at 4 h was the same for both radiopeptides but was a factor of 3 higher than for [^{111}In]−DOTATOC at 2 h (18% vs about 6%). The fast internalization indicates that—according to the current knowledge that only agonistic drugs can internalize (*46*)—[^{67}Ga]− and [^{111}In]−NODAGATOC are both powerful agonists for sstr2 and parallel the improved binding affinity of the two radiopeptides over [^{111}In]−DOTATOC. Internalization was inhibited by the addition of excess octreotide. In the time interval of the study (30 min to 4 h) no steady state was reached yet but the distinct leveling-off indicates the close approach to it which can be explained with the beginning efflux.

If the cells upon internalization of the radioligand for 2 and/or 4 h were exposed to the culture medium, again a time-dependent efflux of the radiopeptides could be observed, indicating a rapid recycling of the radiopeptides to the extracellular medium. A steady state is reached already after 2−4 h of release studies. This is due to the reactivation of the receptor by the released radiopeptide which was shown to be intact by HPLC as it coelutes with the original radiopeptides. It appears that already 25−40% of the externalized agonist are enough to stimulate the receptor to undergo reendocytosis. At steady state, about 60−75% of the radioactivity are located inside the cell and can be routed to lysosomes for degradation. The finding that the amount of externalized radiopeptide and the earlier reaching of a steady state appear to depend on the time internalization was allowed (Figure 3) indicates that this mechanism may be valid. On the other hand, it may just reflect that the steady state is reached earlier because the absolute value of 4 h internalization is higher than the one of 2 h internalization. A distinction between the two possibilities can only be made after careful structural analysis of the peptide contained inside the cells. The interpretation above is in keeping with the conclusion of data obtained by Koenig et al. (*47*), using ^{125}I-labeled somatostatin analogues in sstr2-expressing CHO cells.

Biodistribution Studies. The biodistribution studies in AR4-2J-tumor bearing (sstr2-positive) nude mice showed a higher uptake of [^{67}Ga]−NODAGATOC in sstr-bearing organs and the tumor compared to [^{111}In]−DOTATOC by up to a factor of 2 at 4 h postinjection paralleling the higher binding affinity and higher rate of internalization. Compared to [^{67}Ga]−DOTATOC (data published earlier) the new tracer shows almost the same performance, i.e., a somewhat lower tumor uptake but a higher tumor-to-blood, tumor-to-liver, tumor-to-heart, and a comparable tumor-to-kidney ratio.

In addition, using the same animal model it is far superior to ^{111}In-DTPA-octreotide which showed only 3.03% ± 0.26% ID/g in the tumor at 4 h and an inferior tumor-to-normal organ ratio, e.g. tumor/blood = 7.6, tumor/liver = 4 at the same time point (*28*).

Unforeseen is the fast washout (short residence time) of the tumor and sstr2-positive organs. It is faster compared to other somatostatin-based radiopeptides studied in this laboratory. The approximate biological half-life in the tumor is 7 h. The reason for this is not known yet. Our original hypothesis that it is due to metabolic instability of the exposed peptide bond between NODAGA and D-Phe due to the coupling via the carboxy ethyl spacer compared to the DOTA monoamide coupled peptides was not confirmed by studies with liver homogenate and fresh serum. In the latter cases a protection of the same bond is accomplished due to the fact that the amidocarboxy oxygen is involved in the coordination to the metal. The short tumor retention time resembles somewhat the behavior of most of the [^{64}Cu]−TETA−SRIF analogues discussed by Lewis et al. (*48*). Also, as discussed above, internalization and release studies do not give any clue as to the reason for the fast washout.

In conclusion, NODAGATOC most likely is a peptide−chelator conjugate with very promising properties for human studies if labeled with the short-lived positron emitters ^{68}Ga and ^{66}Ga. Because of the relatively fast washout from tumors, its suitability for a potential therapeutic application with the Auger electron emitter ^{67}Ga has to be shown in other animal models and in patients.

In addition, we developed a new chelator−somatostatin analogue for selective tumor targeting which is also suitable for ^{111}In and because of favorable complex stability most likely for ^{64}Cu and ^{55}Co labeling and their use in the targeting of sstr2-positive tumors in patients.

ACKNOWLEDGMENT

We wish to thank the Swiss National Science Foundation (31-52969.97) and Mallinckrodt Med. for financial support of this work and Novartis for analytical support. M.I.M. Prata acknowledges a grant from Fundaçao Calouste Gulbenkian (Portugal). We are grateful to the group of Prof. Krähenbühl for support with the rat liver homogenate experiment.

LITERATURE CITED

(1) Lamberts, S. W. J., Van der Lely, A.-J., De Herder, W. W., and Hofland, L. J. (1996). Octreotide. *N. Engl. J. Med. 25,* 246−254.

(2) Behr, T. M., Béhé, M., and Becker, W. (1999). Diagnostic applications of radiolabeled peptides in nuclear endocrinology. *Q. J. Nucl. Med. 43,* 268−80.

(3) Fischman, A. J., Babich, J. W., and Strauss, H. W. (1993). A Ticket to Ride: Peptide Radiopharmaceuticals. *J. Nucl. Med. 34,* 2253−2263.

(4) Heppeler, A., Froidevaux, S., Eberle, A. N., and Maecke, H. R. (2000). Receptor Targeting for Tumor Localisation and Therapy with Radiopeptides. *Curr. Med. Chem. 7,* 971−994.

(5) Lister-James, J., Moyer, B. R., and Dean, T. (1996). Small peptides radiolabeld with ^{99m}Tc. *Q. J. Nucl. Med. 40,* 221−233.

(6) Liu, S., and Edwards, D. S. (1999). ^{99m}Tc-Labeled Small Peptides as Diagnostic Radiopharmaceuticals. *Chem. Rev. 99,* 2235−2268.

(7) Reubi, J. C. (1995). Neuropeptide Receptors in Health and Disease: The Molecular Basis for In Vivo Imaging. *J. Nucl. Med. 36,* 1825−35.

(8) Thakur, M. L. (1995). Radiolabeled peptides: Now and the future. *Nucl. Med. Commun. 16,* 724−732.

(9) Krenning, E. P., Bakker, W. H., Kooij, P. P., Breeman, W. A., Oei, H. Y., de Jong, M., Reubi, J. C., Visser, T. J., Bruns, C., and Kwekkeboom, D. J., et al. (1992). Somatostatin receptor scintigraphy with indium-111-DTPA-D-Phe-1-octreotide in man: metabolism, dosimetry and comparison with iodine-123-Tyr^3-octreotide. *J. Nucl. Med. 33,* 652−8.

(10) Krenning, E. P., Kwekkeboom, D. J., Bakker, W. H., Breeman, W. A., Kooij, P. P., Oei, H. Y., van Hagen, M., Postema, P. T., de Jong, M., and Reubi, J. C., et al. (1993). Somatostatin receptor scintigraphy with [^{111}In-DTPA-D-Phe^{1}]- and [^{123}I-Tyr^{3}]-octreotide: the Rotterdam experience with more than 1000 patients. *Eur. J. Nucl. Med. 20,* 716−31.

(11) Heppeler, A., Froidevaux, S., Maecke, H. R., Jermann, E., Béhé, M., Hennig, M., and Powell, P. (1999). Radiometal-Labeled Macrocyclic Chelator-Derivatised Somatostatin Analogue with Superb Tumour-Targeting Properties and Potential for Receptor-Mediated Internal Radiotherapy. *Chem. Eur. J. 5,* 1974−1981.

(12) Smith-Jones, P. M., Stolz, B., Bruns, C., Albert, R., Reist, H. W., Friedrich, R., and Maecke, H. R. (1994). Gallium-67/Gallium-68-[DFO]-Octreotide − A Potential Radiopharmaceutical for PET imaging of Somatostatin Receptor-Positive Tumors: Synthesis and Radiolabeling In Vitro and Preliminary In Vivo Studies. *J. Nucl. Med. 35,* 317−325.

(13) Stolz, B., Smith-Jones, P. M., Albert, R., Reist, H., Maecke, H. R., and Bruns, C. (1994). Biological Characterisation of [^{67}Ga] or [^{68}Ga] Labeled DFO−Octreotide (SDZ 216−297) for PET Studies of Somatostatin Receptor Positive Tumors. *Horm. Metab. Res. 26,* 453−459.

(14) Maecke, H. R., Heppeler, A., and Nock, B. (1999). Somatostatin Analogues Labeled with Different Radionuclides, i*n Technetium, Rhenium and Other Metals in Chemistry and Nuclear Medicine* (M. Nicolini, U. Mazzi, Eds.) Vol. 5, pp 77−91, SGE Ditoriali, Padova.

(15) De Jong, M., Bakker, W. H., Krenning, E. P., Breeman, W. A. P., Pluijm, M. E. v. d., Bernard, B. F., Visser, T. J., Jermann, E., Behe, M., Powell, P., and Maecke, H. R. (1997). Yttrium-90 and indium-111 labeling, receptor binding and biodistribution of [DOTA^{0}, D.-Phe^{1}, Tyr^{3}]octreotide, a promising somatostatin analogue for radionuclide therapy. *Eur. J. Nucl. Med. 24,* 368−371.

(16) Reubi, J. C., Schär, J. C., Waser, B., Wenger, S., Heppeler, A., Schmitt, J. S., and Maecke, H. R. (2000). Affinity profiles for human somatostatin receptor subtypes SST1-SST5 of somatostatin radiotracers selected for scintigraphic and radiotherapeutic use. *Eur. J. Nucl. Med. 27,* 273−282.

(17) Anderson, C. J., and Welch, M. J. (1999). Radiometal-Labeled Agents (Non-Technetium) for Diagnostic Imaging. *Chem. Rev. 99,* 2219−2234.

(18) Green, M. A., Welch, and M. J. (1989). Gallium Radiopharmaceutical Chemistry. *Nucl. Med. Biol. 16,* 435−448.

(19) Caraco, C., Aloj, L., and Eckelman, W. C. (1998). The gallium-deferoxamine complex: stability with different deferoxamine concentrations and incubation conditions. *Appl. Radiat. Isot. 49,* 1477−9.

(20) Sharma, V., Beatty, A., Wey, S. P., Dahlheimer, J., Pica, C. M., Crankshaw, C. L., Bass, L., Green, M. A., Welch, M. J., and Piwnica-Worms, D. (2000). Novel gallium(III) complexes transported by MDR1 P-glycoprotein: potential PET imaging agents for probing P-glycoprotein-mediated transport activity in vivo. *Chem. Biol. 7,* 335−43.

(21) Eisenwiener, K.-P., Powell, P., and Mäcke, H. R. (2000). A Convenient Synthesis of Novel Bifunctional Prochelators for Coupling to Bioactive Peptides for Radiometal Labeling. *Bioorg., Med. Chem. Lett. 10,* 2133−2135.

(22) Atherton, E., and Sheppard, R. (1989). Solid phase peptide synthesis—a practical approach, IRL Press, Oxford.

(23) Reubi, J. C., Kvols, L. K., Waser, B., Nagorney, D. M., Heitz, P. U., Charboneau, J. W., Reading, and C. C., Moertel, C. (1990). Detection of somatostatin receptors in surgical and percutaneous needle biopsy samples of carcinoids and islet cell carcinomas. *Cancer Res. 50,* 5969−77.

(24) Reubi, J. C. (1995). In vitro identification of vasoactive intestinal peptide receptors in human tumors: implications for tumor imaging. *J. Nucl. Med. 36,* 1846−53.

(25) Hofland, L. J., Koetsveld, P. M. v., Waaijers, M., Zuydenrwijk, J., Breeman, W. A. P., Krenning, E. P., and Lamberts, S. W. J. (1995). Internalization of the radioiodinated somatostatine analogue [^{125}I-Tyr^{3}]octreotide by mouse and human pituitary tumor cells: increase by unlabeled octreotide. *Endocrinology 136,* 3698−3706.

(26) De Jong, M., Bernard, B. F., Brun, E. d., Gameren, A. v., Bakker, W. H., Visser, T. J., Mäcke, H. R., and Krenning, E. P. (1998). Internalization of radiolabeled [DTPA°]octreotide and [DOTA, Tyr^{3}]octreotide: peptides for somatostatine receptor-targeted scintigraphy and radionuclide therapy. *Nucl. Med. Commun. 19,* 283−288.

(27) Arano, Y., Akizawa, H., Uezono, T., Akaji, K., Ono, M., Funakoshi, S., Koizumi, M., Yokoyama, A., Kiso, Y., and Saji, H. (1997). Conventional and high-yield synthesis of DTPA-conjugated peptides: application of a monoreactive DTPA to DTPA-D-Phe^{1}-octreotide synthesis. *Bioconjugate Chem. 8,* 442−446.

(28) Froidevaux, S., Heppeler, A., Eberle, A. N., Meier, A.-M., Häusler, M., Beglinger, C., Béhé, M., Powell, P., and Mäcke, H. R. (2000). Preclinical Comparison in AR4-2J Tumor Bearing-Mice of Four Radiolabeled 1,4,7,10-Tetraazacyclododecane-1,4,7,10-Tetraacetic Acid-Somatostatin Analogues for Tumor Diagnosis and Internal Radiotherapy. *Endocrinology 141,* 3304−3312.

(29) Anderson, C. J., Dehdashti, F., Cutler, P. D., Schwarz, S. W., Laforest, R., and Bass, L. A., et al. (2001). ^{64}Cu-TETA-octreotide as a PET imaging agent for patients with neuroendocrine tumors. *J. Nucl. Med. 42,* 213−21.

(30) Anderson, C. J., Pajeau, T. S., Edwards, W. B., Sherman, E. L. C., Rogers, B. E., and Welch, M. J. (1995). In Vitro and In Vivo Evaluation of Copper-64-Octreotide Conjugates. *J. Nucl. Med. 36,* 2315−2325.

(31) Lewis, J. S., Srinivasan, A., Schmidt, M. A., and Anderson, C. J. (1999). In vitro and in vivo evaluation of ^{64}Cu-TETA-Tyr^{3}-octreotate. A new somatostatin analogue with improved target tissue uptake. *Nucl. Med. Biol. 26,* 267−73.

(32) Wester, H.-J., Brockmann, J., Rösch, F., Wurz, W., Herzog, H., Smith-Jones, P., Stolz, B., Bruns, C., and Stöcklin, G. (1997). PET-Pharmacokinetics of ^{18}F−Octreotide: A Comparison with ^{67}Ga-DFO and ^{86}Y-DTPA-Octreotide. *Nucl. Med. Biol. 24,* 275−286.

(33) Förster, G. J., Engelbach, M., Brockmann, J., Reber, H., Buchholz, H.-G., Mäcke, H. R., Rösch, F., Herzog, H., and Bartenstein, P. (2001). Preliminary data on biodistribution and dosimetry for therapy planning of somatostatin receptor positive tumours: comparison of ^{86}Y-DOTATOC and ^{111}In-DTPA-octreotide. *Eur. J. Nucl. Med. 28/12,* 1743−1750.

(34) Henze, M., Schuhmacher, J., Hipp, P., Kowalski, J., Becker, D. W., Doll, J., Mäcke, H. R., Hofmann, M., Debus, J., and Haberkorn, U. (2001). PET Imaging of Somatostatin Receptors Using [^{68}Ga]DOTA-D-Phe^{1}-Tyr^{3}-Octreotide: First Results in Patients with Meningiomas. *J. Nucl. Med. 42,* 1053−1056.

(35) Hofmann, M., Maecke, H. R., Börner, A. R., Weckesser, E., Schöffski, P., Oei, M. L., Schumacher, J., Henze, M., Heppeler, A., Meyer, G. J., and Knapp, W. H. (2001). Biokinetics and imaging with the somatostatin receptor PET radioligand ^{68}Ga-DOTATOC: preliminary data. *Eur. J. Nucl. Med. 28/12,* 1751−1757.

(36) McMurry, T. J., Brechbiel, M., Wu, C., and Gansow, O. A. (1993). Synthesis of 2-(p-Thiocyanatobenzyl-1,4,7-triazacyclononane-1,4,7-triacetic Acid: Application of the 4-Methoxy-2,3,6-trimethylbenzenesulfonamide Protecting Group in the Synthesis of Macrocyclic Polyamines. *Bioconjugate Chem. 4,* 236−245.

(37) Cox, J. P. L., Craig, A. S., Helps, I. M., Jankowsi, K. J., Parker, D., Eaton, M. A. W., Millican, A. T., Millar, K., Beeley, N. R. A., and Boyce, B. A. (1990). Synthesis of C- and N−Functionalised Derivatives of 1,4,7-Triazacyclononane-1,4,7-triacetic Acid (NOTA), 1,4,7,10-Tetra-azacyclododecane-1,4,7,10-tetrayltetraacetic Acid (DOTA), and Diethylenetriaminepenta-acetic Acid (DTPA): Bifunctional Complexing Agents for the Derivatisation of Antibodies. *J. Chem. Soc., Perkin Trans. 1* 2567−76.

(38) Studer, M., and Meares, C. F. (1992). Synthesis of Novel 1,4,7-Triazacyclononane-*N*,*N*′,*N*″-triacetic Acid Derivatives Suitable for Protein Labeling. *Bioconjugate Chem. 3,* 337−341.

(39) Brechbiel, M., McMurry, T. J., and Gansow, O. A. (1993). A Direct Synthesis of a Bifunctional Chelating Agent for Radiolabeling Proteins. *Tetrahedron Lett. 34,* 3691−3694.

(40) Chappell, L. L., Rogers, B. E., Khazaeli, M. B., Mayo, M. S., Buchsbaum, D. J., and Brechbiel, M. W. (1999). Improved Synthesis of the Bifunctional Chelating Agent 1, 4,7,10-Tetraaza-N-(1-carboxy-3-(4-nitrophenyl)propyl)-N′,N″,N‴-tris(acetic acid)cyclododecane (PA-DOTA). *Bioorg. Med. Chem. 7,* 2313−2320.

(41) Kruper, W. J., Rudolf, P. R., and Langhoff, C. A. (1993). Unexpected Selectivity in the Alkylation of Polyazamacrocycles. *J. Org. Chem. 58,* 3869−3876.

(42) André, J. P., Mäcke, H. R., Zehnder, M., Macko, L., and Acyel, K. G. (1998). 1,4,7-Triazacyclononane-1-succinic acid-4,7-diacetic acid (NODASA): a new bifunctional chelator for radio gallium-labeling of biomolecules. *Chem. Commun.* 1301−1302.

(43) Shannon, R. D. (1976). Revised Effective Ionic Radii and Systematic Studies of Interatomic Distances in Halides and Chalcogenides. *Acta Crystallogr. 32 A,* 751−767.

(44) Broan, C. J., Cox, J. P. L., Craig, A. S., Kataky, R., Parker, D., Harrison, A., Randall, A. M., and Ferguson, G. (1991). Structure and Solution Stability of Indium and Gallium Complexes of 1,4,7-Triazacyclononanetriacetate and of Yttrium Complexes of of 1,4,7,10-Tetraazacyclododecanetetraacetate and Related Ligands: Kinetically Stable Complexes for Use in Imaging and Radioimmunotherapy. X-ray Molecular Structure of the Indium and Gallium Complexes of 1,4,7-Triazacyclononane-1,4,7-triacetic Acid. *J. Chem. Soc., Perkin Trans. 2,* 87−98.

(45) Clarke, E. T., Martell, A. (1991). Stabilities of the Fe(III), Ga(III) and In(III) chelates of N,N′,N″-triazacyclononanetriacetic acid. *Inorg. Chim. Acta 181,* 273−280.

(46) Koenig, J. A., and Edwardson, J. M. (1997). Endocytosis and recycling of G protein-coupled receptors. *Trends Pharmacol. Sci.* 276−287.

(47) Koenig, J. A., Kaur, R., Dodgeon, I., Edwardson, J. M., and Humphrey, P. P. A. (1998). Fates of endocytosed somatostatin sst2 receptor and associated agonists. *Biochem. J. 336,* 291−298.

(48) Lewis, J. S., Lewis, M. R., Srinivasan, A., Schmidt, M. A., Wang, J., and Anderson, C. J. (1998). Comparison of Four ^{64}Cu-Labeled Somatostatin Analogues in Vitro and in Tumor-Bearing Rat Model: Evaluation of New Derivatives for Positron Emission Tomography Imaging and Targeted Radiotherapy. *J. Med. Chem.* 1341−1347.

BC010074F